Improved Selective Harmonics Elimination Scheme With Online Harmonic Compensation for High-Power PWM Converters

Ye Zhang, *Student Member, IEEE*, Yun Wei Li, *Senior Member, IEEE*, Navid R. Zargari, *Senior Member, IEEE*, and Zhongyuan Cheng, *Member, IEEE*

***Abstract*—To reduce the low-order harmonics produced by the high-power pulsewidth-modulated (PWM) converters, selective harmonic elimination (SHE) scheme is commonly used due to its superior harmonic performance at low switching frequency. However, as an off-line modulation technique, the SHE scheme itself lacks the capability to realize the active compensation of the grid background harmonics. To enable the active compensation ability of the SHE-modulated PWM converters, this paper proposes an active compensation method through the jittering of SHE phase angle. The proposed method can realize the real-time compensation of the preexisting system background harmonics in high-power PWM converters' system. An application example on a high-power PWM current-source rectifier (CSR) system is provided in this paper. Experimental results show that the proposed method can effectively attenuate the line current harmonics caused by the grid background harmonics in the high-power PWM CSR systems.**

***Index Terms*—Current-source rectifier (CSR), harmonic compensation, high-power converter, real-time compensation, selective harmonic elimination (SHE).**

I. Introduction

HIGH-POWER converters, such as multilevel voltage-source converters and current-source converters, are widely used in high-power (>1 MVA) medium-voltage (2.3–13.8 kV) ac drives, HVDC systems, etc. Typically, the high-power converters are operated with a low switching frequency (300–800 Hz) in order to reduce the switching power loss [1]. The low switching frequency is prone to produce low-order harmonics, which may cause significant line current distortion due to the converter system's filter circuit. To avoid such problems, the selective harmonic elimination (SHE) modulation scheme is commonly adopted at the high-power pulsewidth-modulated (PWM) converters due to its superior harmonic performance at low switching frequency. Taking a high-power PWM current-source rectifier (CSR) system as shown in Fig. 1; for example, a three-phase capacitor is required at the rectifier input to assist the commutation of switching devices, which forms an *LC* filter with the grid line impedance and filter reactor. Considering the CSR switching frequency and the input power factor, the commutation capacitance is commonly sized between 0.3 and 0.5 p.u. [1], [2]. As the total line inductance (grid line inductance and filter inductance) is normally in the range of 0.1–0.15 p.u., the resultant *LC* resonant frequency is within 3.6–5.8 p.u. so that the low-order harmonics (such as 5th) produced by the PWM CSR may result in significant line current distortion [2]. Considering this potential problem, the PWM CSR is commonly modulated by the SHE scheme [3]–[6]. A typical control diagram of high-power PWM CSR system is shown in Fig. 2, where the dc-link current is controlled by delay angle (α).

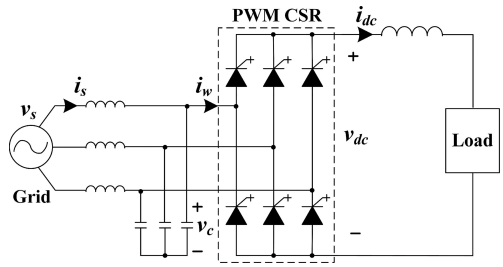

Fig. 1. Topology of PWM CSR system.

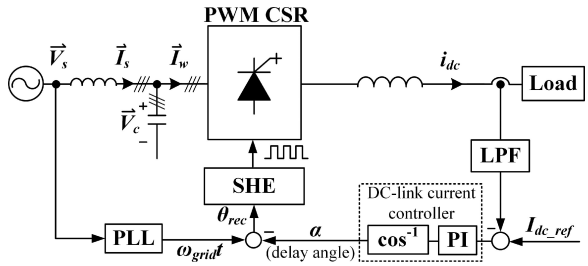

Fig. 2. Typical control diagram of high-power PWM CSR system.

Nevertheless, as an off-line technique, the SHE scheme itself lacks the capability to actively attenuate the current distortion caused by the system background harmonics (e.g., the significant line current distortion may be resulted from the low-order grid voltage harmonics, such as 5th, in PWM CSR system due to the *LC* filter) [2]. On the one hand, since the modulation index (m_a) is fixed in a fundamental cycle of SHE PWM pattern, the $m_a - based$ active damping methods [2], [7]–[14] cannot be applied based on the SHE scheme. On the other hand, the constraint of quarter-wave symmetry in SHE scheme confines all

Manuscript received January 26, 2014; revised July 16, 2014; accepted July 22, 2014. Date of publication August 7, 2014; date of current version February 13, 2015. This paper will be presented in part at the IEEE Energy Conversion Congress and Exposition, Pittsburgh, PA, USA, 2014. Recommended for publication by Associate Editor J. H. R. Enslin.

Y. Zhang and Y. W. Li are with the Department of Electrical and Computer Engineering, University of Alberta, Edmonton, AB T6G 2V4, Canada (email: ye17@ualberta.ca; yunwei.li@ualberta.ca).

N. R. Zargari and Z. Cheng are with the Medium Voltage R&D Department, Rockwell Automation Canada Inc., Cambridge, ON N1R 5X1, Canada (e-mail: nrzargari@ra.rockwell.com; gcheng@ra. rockwell.com).

Color versions of one or more of the figures in this paper are available online at http://ieeexplore.ieee.org.

Digital Object Identifier 10.1109/TPEL.2014.2345051

the harmonics in PWM pattern to be either in phase or antiphase with the fundamental [15]–[17], which means that the phase of each harmonic is uncontrollable. To enable the active compensation capability of the SHE-modulated PWM converters, Zhou *et al*. [18] proposed a selective harmonics compensation (SHC) PWM scheme by relaxing the quarter-wave symmetry in SHE scheme so that both the magnitude and the phase angle of each order harmonic in PWM pattern can be controlled. In the SHC scheme, different sets of switching angles are off-line calculated to generate the different magnitude and phase angle of certain harmonics in PWM pattern. The sets of switching angles are saved in a lookup table and selected according to the expected harmonics in PWM pattern during the online implementation. Based on the SHC scheme, Zhou *et al.* [18] and Ni *et al.* [19] realized the active attenuation of line current harmonics caused by the grid voltage harmonics in high-power PWM CSR system. Although the SHC scheme can enable the active compensation capability of the high-power converters, it has some drawbacks in applications. At first, a considerable off-line calculation is needed to create the lookup table and a compromise has to be made between the resolution and the size of the table. In addition, a multidimensional table will be required to actively compensate more than one harmonic that challenges both the calculation and the storage. Moreover, since the switching angles can only be updated once in a fundamental cycle during the online implementation, up to one fundamental delay will be introduced which may affect the compensation performance.

To overcome the aforementioned drawbacks, an improved SHE scheme with online harmonic compensation is proposed in this paper. This method actively produces the expected harmonics in SHE PWM pattern through introducing a compensation signal in SHE phase angle, and such a compensation signal can be obtained by a simple algebraic calculation. It not only saves the effort on creating the lookup table but also realizes the real-time active compensation of high-power converters. In this paper, an implementation example of the improved-SHE-scheme-based active compensation to attenuate line current harmonics in high-power PWM CSR system is provided, and experimental results verify its effectiveness.

II. Basic Principle of Improved SHE Scheme With Online Harmonic Compensation

Define the phase angle of SHE pattern as θ. At steady state, θ will repeatedly increase from 0 to 2π at system fundamental frequency ω, which can be represented by $\theta = \omega t + \varphi$ (φ is the initial phase). For example, in the PWM CSR system shown in Fig. 2, θ is equal to $\theta_{rec}(\theta_{rec} = \omega_{grid}t–\alpha)$, which varies from 0 to 2π repeatedly with 60 Hz grid fundamental frequency at steady state.

Then, the *h*th harmonic in SHE pattern $\vec{S}_{wh}$ can be represented as (defined in *sine* system)

$$\begin{aligned}\vec{S}_{wh} &= -jM_{sh}e^{j(h\theta+\varphi_{sh})} \\ &= -jM_{sh}e^{j(h(\omega t+\varphi)+\varphi_{sh})} \quad (h = 1, -5, 7, -11, 13, \ldots)\end{aligned} \tag{1}$$

where M_{sh} and φ_{sh} are the magnitude and the initial phase of the *h*th harmonic, respectively. In (1), the positive *h* represents the positive sequence and the negative *h* represents the negative sequence. When *h* is negative, $M_{sh} = –M_{s(-h)}$ and $\varphi_{sh} = –\varphi_{s(-h)}$.

Introducing an ω_{comp}-frequency alternating signal $\theta_{comp} = M_{comp}sin(\omega_{comp}t + \varphi_{comp})$ into θ, the SHE phase angle can be represented as

$$\theta' = \theta + \theta_{comp} = (\omega t + \varphi) + M_{comp}\sin(\omega_{comp}t + \varphi_{comp}) \tag{2}$$

where M_{comp} and φ_{comp} are the magnitude and the initial phase of θ_{comp}, respectively. Then, the *h*th harmonic in SHE pattern $\vec{S}_{wh}$ shown in (1) is rewritten as

$$\vec{S}_{w}^{\mathrm{SHE}_h} = -jM_{sh}e^{j(h(\omega t+\varphi+M_{comp}\sin(\omega_{comp}t+\varphi_{comp}))+\varphi_{sh})}. \tag{3}$$

Taking Jacobi–Anger extension of (3) [20], we can obtain that

$$\begin{aligned}\vec{S}_{w}^{\mathrm{SHE}_h} &= -jJ_0\left(hM_{comp}\right)M_{sh}e^{j(h(\omega t+\varphi)+\varphi_{sh})} \\ &\quad -j\sum_{k=1}^{\infty}J_k\left(hM_{comp}\right) \\ &\quad \times M_{sh}e^{j((h\omega+k\omega_{comp})t+h\varphi+\varphi_{sh}+k\varphi_{comp})} \\ &\quad -j\sum_{k=1}^{\infty}(-1)^k J_k\left(hM_{comp}\right) \\ &\quad \times M_{sh}e^{j((h\omega-k\omega_{comp})t+h\varphi+\varphi_{sh}-k\varphi_{comp})}\end{aligned} \tag{4}$$

where $J_k(\cdot)$ is the Bessel function. Comparing (4) with (1), we can observe that, after introducing θ_{comp}, the sideband harmonics are produced at each ω_{comp} interval around the original *h*th harmonic in PWM pattern. For each sideband component, its magnitude ($|J_k(hM_{comp})M_{sh}|$), frequency ($|h\omega \pm k\omega_{comp}|$), and initial phase ($h\varphi + \varphi_{sh} \pm k\varphi_{comp}$) are the independent function of the magnitude (M_{comp}), frequency (ω_{comp}), and initial phase (φ_{comp}) of θ_{comp}, respectively. It means that the sideband harmonics can be controlled by θ_{comp}, which provides a possibility to produce the expected harmonics in PWM pattern based on the SHE scheme to realize the active harmonic compensation. The diagram of $\vec{S}_{wh}$ and $\vec{S}_{w}^{\mathrm{SHE}_h}$ can be sketched as Fig. 3.

According to the earlier analysis, the basic operation principle of the proposed method is to produce the expected harmonics in PWM pattern by changing the predefined SHE pattern online through the jittering of its phase angle, which can be illustrated as shown in Fig. 4. In Fig. 4, θ_{sw1}, θ_{sw2}, θ_{sw3}, …, are the predesigned switching angles in SHE pattern, and by comparing θ with θ_{sw}, the SHE PWM pattern is generated as shown in the left plot of Fig. 4. For the improved SHE scheme with online harmonic compensation as shown in the right plot of Fig. 4, an alternating signal θ_{comp} is introduced into θ that forms a new SHE phase angle θ'. By comparing the jittering θ' with θ_{sw}, the SHE pattern is altered online so as to produce the expected harmonics in PWM pattern.

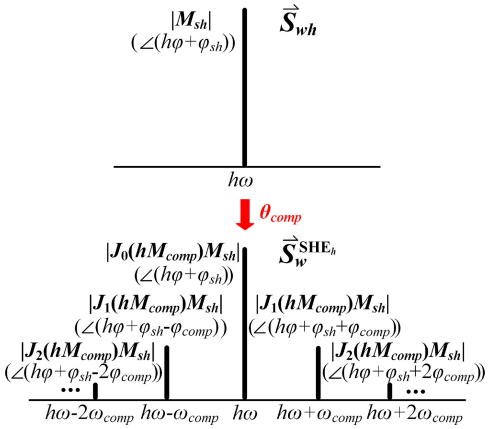

Fig. 3. Diagram of $\vec{S}_{wh}$ and $\vec{S}_w^{\mathrm{SHE}_h}$.

III. SHC-Scheme-Based Active Compensation in High-Power PWM CSR Systems

In order to illustrate the advantages of the proposed improved SHE scheme over the previous SHC scheme, an example of the SHC scheme adopted to actively attenuate the line current harmonics in high-power PWM CSR systems is provided in this section, and a detailed discussion of its drawbacks is presented. Then in the next section, the proposed improved SHE scheme with online harmonic compensation will be implemented under the same situation of the system.

Based on the SHC scheme, Zhou *et al*. [18] and Ni *et al*. [19] realized the active attenuation of the negative-sequence 5th line current harmonic caused by the utility harmonics in PWM CSR system. Fig. 5 shows the diagram of attenuation method presented in [19]. Through multiplying the measured negative-sequence 5th line current harmonic ($\vec{I}_{s(-5)}$) by a designed coefficient K_v, the reference of 5th PWM current harmonic ($\vec{I}^{\,*}_{w(-5)}$) is generated by a grid-side virtual impedance strategy and then sent to the SHC PWM scheme. In the SHC scheme, dividing $\vec{I}^{\,*}_{w(-5)}$ by the dc-link current reference I_{dc_ref}, the magnitude reference M^*_{s5} and phase reference φ^*_{s5} of 5th harmonic in PWM pattern $\vec{S}^{\,*}_{w(-5)}$ are obtained and input into a two-dimensional lookup table thereafter. The sets of switching angles saved in the lookup table are off-line calculated with respect to the different magnitude and phase reference of 5th harmonic in PWM pattern. In online implementation, according to M^*_{s5} and φ^*_{s5}, the lookup table indexes the corresponding switching angles once every fundamental cycle to generate the 5th PWM current harmonic $\vec{I}_{w(-5)}$ through the PWM CSR.

As described previously, at first, a considerable off-line calculation of trigonometric equation sets is required to create the lookup table and a tradeoff between the resolution and the size has to be made. In addition, according to Fig. 5, a four-dimensional lookup table will be required to actively attenuate two line current harmonics (such as 5th and 7th) which challenges both the calculation and the storage during the implementation. For the calculation, not only the amount and complexity of nonlinear equations will be greatly increased, but also the solution becomes harder to be obtained. For the storage, if the lookup table used in [18] and [19] is extended to four dimensions with the same resolution, around 230 MB memory space will be needed which greatly challenges the real implementation. Moreover, since the switching angles can only be updated once in a fundamental cycle, the magnitude and phase angle of the produced 5th harmonic in PWM pattern will be fixed within one fundamental cycle. As a result, in the worst case, one fundamental delay may be caused in the attenuation of line current harmonics which will affect the compensation performance.

IV. Active Compensation Based on Improved SHE Scheme in High-Power PWM CSR Systems

As discussed in previous section, to attenuate the 5th line current harmonic, Zhou *et al* [18] and Ni *et al.* [19] utilized the SHC scheme to generate the 5th PWM current harmonic $\vec{I}_{w(-5)}$ according to the reference $\vec{I}^{\,*}_{w(-5)}$. To overcome the aforementioned disadvantages of SHC scheme, the proposed improved SHE scheme with online harmonic compensation can be adopted to produce $\vec{I}_{w(-5)}$ according to $\vec{I}^{\,*}_{w(-5)}$.

If we neglect the influence of harmonics in SHE pattern but only consider the fundamental component, according to (1) ($h = 1$, $M_{s1} \approx 1$, $\varphi_{s1} = 0$), we can obtain (5) with respect to the PWM CSR system ($\theta = \theta_{rec} = \omega_{grid}t - \alpha$ as discussed in Section II)

$$\vec{S}_{w1} = -je^{j(\omega_{grid}t-\alpha)}. \tag{5}$$

Then, according to (4), (6) can be obtained after introducing θ_{comp}

$$\begin{aligned}\vec{S}_w^{\mathrm{SHE}_1} = & -jJ_0\left(M_{comp}\right)e^{j(\omega_{grid}t-\alpha)} \\ & -j\sum_{k=1}^{\infty}J_k\left(M_{comp}\right) \\ & \times e^{j((\omega_{grid}+k\omega_{comp})t-\alpha+k\varphi_{comp})} \\ & -j\sum_{k=1}^{\infty}(-1)^k J_k\left(M_{comp}\right) \\ & \times e^{j((\omega_{grid}-k\omega_{comp})t-\alpha-k\varphi_{comp})}.\end{aligned} \tag{6}$$

.

When M_{comp} is small, based on the Bessel function properties shown in Figs. 6–8, (7)–(9) can be obtained

$$J_0\left(M_{comp}\right) \approx 1 \tag{7}$$

$$J_1\left(M_{comp}\right) \approx \frac{1}{2}M_{comp} \tag{8}$$

$$J_k\left(M_{comp}\right) \approx 0 (k \geq 2). \tag{9}$$

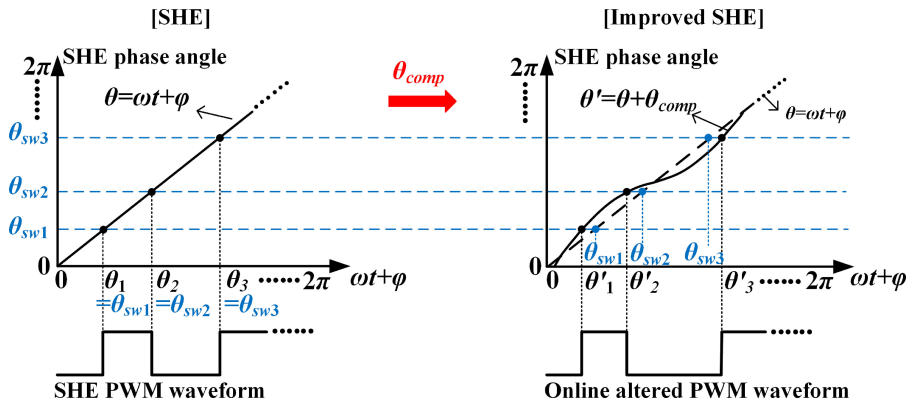

Fig. 4. Illustration of the basic operation principle of the improved SHE scheme with online harmonic compensation.

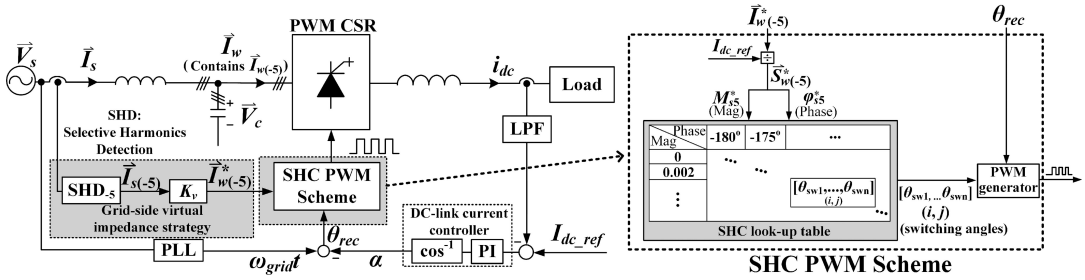

Fig. 5. Diagram of the 5th line current harmonic attenuation in PWM CSR system presented in [19].

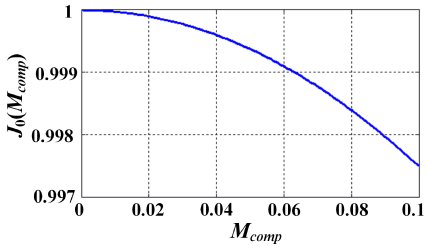

Fig. 6. $J_0(M_{comp})$ versus M_{comp}.

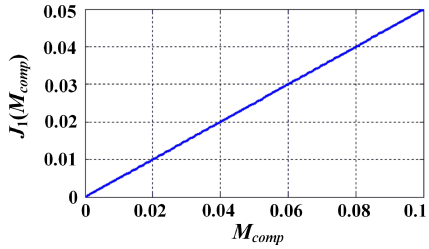

Fig. 7. $J_1(M_{comp})$ versus M_{comp}.

Substituting (7)–(9) into (6), we can obtain that

$$\begin{aligned}\vec{S}_w^{\mathrm{SHE}_1} \approx & -je^{j(\omega_{grid}t-\alpha)} \\ & +j\frac{1}{2}M_{comp}e^{-j((\omega_{comp}-\omega_{grid})t+\alpha+\varphi_{comp})} \\ & -j\frac{1}{2}M_{comp}e^{j((\omega_{comp}+\omega_{grid})t-\alpha+\varphi_{comp})}. \quad (10)\end{aligned}$$

It can be observed that (10) contains three components, which are the fundamental component, the left nearest, and the right nearest sideband harmonic introduced by θ_{comp}, respectively. By selecting $\omega_{comp} = 6\omega_{grid}$, such three components can be represented as $\vec{S}_{w1}^{\mathrm{SHE}_1}$, $\vec{S}_{w(-5)}^{\mathrm{SHE}_1}$, and $\vec{S}_{w7}^{\mathrm{SHE}_1}$, respectively, shown in (11)

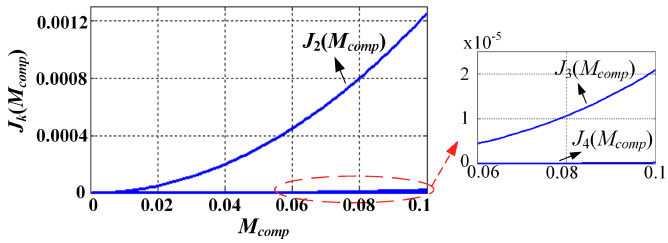

Fig. 8. $J_k(M_{comp})$ versus $M_{comp}(k \geq 2)$.

$$\begin{cases}\vec{S}_{w1}^{\mathrm{SHE}_1} = -je^{j(\omega_{grid}t-\alpha)} \\ \vec{S}_{w(-5)}^{\mathrm{SHE}_1} = +j\frac{1}{2}M_{comp}e^{-j(5\omega_{grid}t+\alpha+\varphi_{comp})} \\ \vec{S}_{w7}^{\mathrm{SHE}_1} \approx -j\frac{1}{2}M_{comp}e^{j(7\omega_{grid}t-\alpha+\varphi_{comp})}.\end{cases} \quad (11)$$

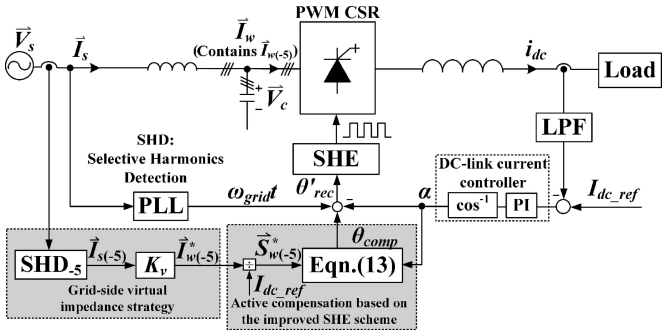

Fig. 9. Diagram of the 5th line current harmonic attenuation by adopting the improved-SHE-scheme-based active compensation.

To generate $\vec{I}_{w(-5)}$, $\vec{S}^{\mathrm{SHE}_1}_{w(-5)}$ in (11) can be used to produce $\vec{S}^{*}_{w(-5)}$ shown in Fig. 5. As shown in Fig. 5, $\vec{S}^{*}_{w(-5)}$ is obtained by (12). Then, to realize $\vec{S}^{\mathrm{SHE}_1}_{w(-5)} = \vec{S}^{*}_{w(-5)}$, (13) is derived.

$$\vec{S}^{*}_{w(-5)} = \frac{\vec{I}^{*}_{w(-5)}}{I_{dc\_ref}} = jM^{*}_{s5}e^{-j(5\omega_{grid}t+\varphi^{*}_{s5})} \tag{12}$$

$$\begin{cases} M_{comp} = 2M^{*}_{s5} \\ \varphi_{comp} = \varphi^{*}_{s5} - \alpha \end{cases} \tag{13}$$

By using the grid-side virtual impedance strategy shown in Fig. 5, the diagram of the 5th line current harmonic attenuation based on the improved SHE scheme with online harmonic compensation can be drawn as shown in Fig. 9.

With respect to the active compensation based on the improved SHE scheme, the following features are offered:

1) *Real-time active compensation*: As shown in Fig. 9, to generate $\vec{I}_{w(-5)}$ through the improved SHE scheme, only a simple algebraic calculation as shown in (13) is needed. Not only will it save the effort on creating the SHC lookup table, but also the real-time active compensation based on the SHE scheme is realized without introducing any delay due to the update of switching angles in SHC scheme. Furthermore, if it is combined with the SHC scheme to attenuate two line current harmonics (e.g., the proposed method is used to attenuate the 5th line current harmonic; the SHC scheme is used to attenuate the 7th line current harmonic), only a two-dimensional lookup table will be needed instead of the four-dimensional table when only adopting the SHC scheme as mentioned previously.
2) *No influence on dc-link current control*: According to (5) and (11), the fundamental component $\vec{S}^{\mathrm{SHE}_1}_{w1}$ in (11) is the same as $\vec{S}_{w1}$ in (5), which means that θ_{comp} will not change the fundamental component in PWM pattern. Since the dc-link current control is only related to the fundamental component in PWM pattern at steady state, the improved-SHE-scheme-based active compensation will not affect the dc-link current control in PWM CSR system.
3) *No increase on pulse numbers of PWM waveforms:* Since the delay angle α is constant at steady state, the SHE phase angle θ_{rec} will be an increasing function from 0 to 2π as discussed in Section II. For the new SHE phase angle θ'_{rec} after introducing θ_{comp}, according to (2), we can obtain (14), and it will be greater than zero (increasing function) if $M_{comp} < \omega_{grid}/\omega_{comp}$

$$\frac{\mathrm{d}\theta'_{rec}}{\mathrm{d}t} = \omega_{grid} + \omega_{comp}M_{comp}\cos(\omega_{comp}t + \varphi_{comp}). \tag{14}$$

Based on (14), if we could confine $M_{comp} < 1/6$ during the attenuation of the 5th line current harmonic ($\omega_{comp} = 6\omega_{grid}$), the jittering of SHE phase angle after introducing θ_{comp} will not affect its increasing function properties. As a result, the proposed improved SHE scheme will not increase the pulse numbers of PWM waveforms.

Regarding the attenuation of the 5th line current harmonic developed in this section, one possible complication is that the parasitic 7th harmonic $\vec{S}^{\mathrm{SHE}_1}_{w7}$ is also produced in PWM pattern besides $\vec{S}^{\mathrm{SHE}_1}_{w(-5)}$ used in compensation as can be seen from (11). Such 7th harmonic may distort the 7th line current harmonic. However, with a small θ_{comp}, its influence on 7th line current harmonic is insignificant, especially considering the attenuation effect of the grid-side *LC* circuit. This is verified in the experimental results.

V. Influence of Harmonics in SHE Pattern on the Improved-SHE-Scheme-Based Active Compensation

In Section IV, the improved-SHE-scheme-based active compensation is derived without considering the harmonics in SHE pattern. However, according to (4), the harmonics in SHE pattern will also generate the sideband harmonics after introducing the compensation signal θ_{comp} in SHE phase angle. It may affect the dc-link current control, or degrade the compensation of line current harmonics, or increase the other line current harmonics. At first, to attenuate the 5th line current harmonic ($\omega_{comp} = 6\omega_{grid}$), the right nearest sideband component of negative-sequence 5th harmonic in SHE pattern, the left nearest sideband component of positive-sequence 7th harmonic in SHE pattern, and etc., are all at the fundamental frequency according to Fig. 3, which may affect the dc-link current control after introducing θ_{comp}. In addition, the right nearest sideband component of negative-sequence 11th harmonic in SHE pattern, the second right nearest sideband component of negative-sequence 17th harmonic in SHE pattern, etc., are all at the negative-sequence 5th order, which may degrade the performance of 5th line current harmonic attenuation. Moreover, the sideband components of harmonics in SHE pattern at other low orders, such as 7th and 11th, may increase the corresponding line current harmonics. To reduce the aforementioned influence of the sideband harmonics produced by the SHE harmonics and θ_{comp}, besides the adoption of small M_{comp} as discussed previously, the design of SHE pattern is needed to be analyzed. Table I shows the influence of the harmonics in SHE pattern on the PWM pattern after introducing θ_{comp}. In Table I, the row represents the *h*th harmonic in SHE pattern; the column represents the *k*th harmonic in PWM pattern after introducing θ_{comp}; the table contents are the magnitude of the *k*th harmonic in PWM pattern generated by

TABLE I
INFLUENCE OF THE HARMONICS IN SHE PATTERN ON THE PWM PATTERN AFTER INTRODUCING θ_{comp}

Magnitude ($\left\vec{S}_{wk}^{\mathrm{SHE}_h}\right\vert$)		PWM Pattern After Introducing $\theta_{comp}(k)$			
		1st	5th	7th	11th
SHE Pattern (h)	5th	$J_1(5M_{comp})M_{s5}$	$J_0(5M_{comp})M_{s5}$	$J_2(5M_{comp})M_{s5}$	$J_1(5M_{comp})M_{s5}$
	7th	$J_1(7M_{comp})M_{s7}$	$J_2(7M_{comp})M_{s7}$	$J_0(7M_{comp})M_{s7}$	
	11th	$J_2(11M_{comp})M_{s11}$	$J_1(11M_{comp})M_{s11}$		$J_0(11M_{comp})M_{s11}$
	13th	$J_2(13M_{comp})M_{s13}$		$J_1(13M_{comp})M_{s13}$	
	17th		$J_2(17M_{comp})M_{s17}$		$J_1(17M_{comp})M_{s17}$
	19th			$J_2(19M_{comp})M_{s19}$	

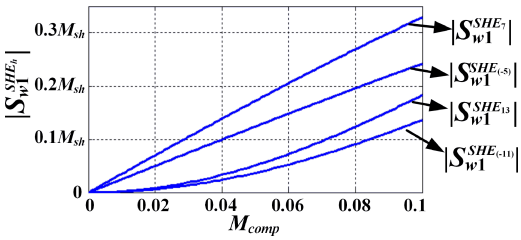

Fig. 10. $\left\vec{S}_{w1}^{\mathrm{SHE}_h}\right\vert$ versus M_{comp}.

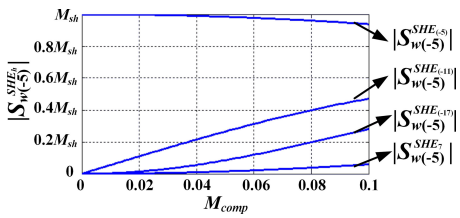

Fig. 11. $\left\vec{S}_{w(-5)}^{\mathrm{SHE}_h}\right\vert$ versus M_{comp}.

the hth harmonic in SHE pattern after introducing θ_{comp} which is represented by $\left\vec{S}_{wk}^{\mathrm{SHE}_h}\right\vert$. The high-order harmonics (>11th) in PWM pattern after introducing θ_{comp} are not considered as they have less influence on line current harmonics due to the *LC* filter, and only the left two nearest and right two nearest side-band components of the harmonics in SHE pattern are taken into account. According to Table I, $\left\vec{S}_{w1}^{\mathrm{SHE}_h}\right\vert$, $\left\vec{S}_{w(-5)}^{\mathrm{SHE}_h}\right\vert$, $\left\vec{S}_{w7}^{\mathrm{SHE}_h}\right\vert$, and $\left\vec{S}_{w(-11)}^{\mathrm{SHE}_h}\right\vert$ versus M_{comp} are drawn as shown in. According to Figs. 10–13, to reduce the influence of harmonics in SHE pattern as mentioned earlier, the SHE pattern is expected to be designed as:

1) Fully eliminate 5th and 7th harmonics.
2) Greatly mitigate 11th and 13th harmonics.
3) Reduce 17th and 19th harmonics as much as possible.

It can be observed that the listed design criteria of SHE pattern are similar as the traditional SHE scheme which is aiming to fully eliminate the low-order harmonics. The experimental results demonstrate that the proposed method can actively attenuate the 5th line current harmonic based on the traditional SHE scheme.

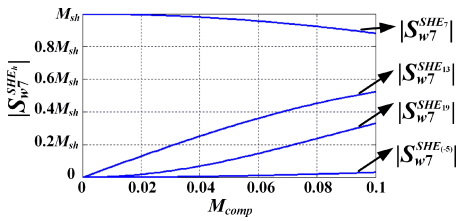

Fig. 12. $\left\vec{S}_{w7}^{\mathrm{SHE}_h}\right\vert$ versus M_{comp}.

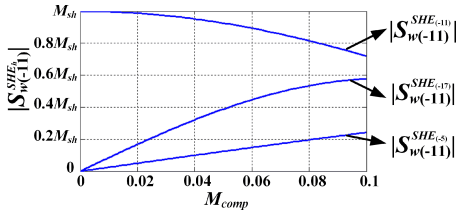

Fig. 13. $\left\vec{S}_{w(-11)}^{\mathrm{SHE}_h}\right\vert$ versus M_{comp}.

TABLE II
PARAMETERS OF EXPERIMENTAL SYSTEM

Parameters	**Values**
Rated power	10 kVA
Rated voltage (line to line)	208 V
Grid-side line inductance	1.67 mH (0.15 p.u.)
Grid-side filter capacitance	240 μF (0.40 p.u.)
DC-link choke	10 mH (0.58pu)
DC-link resistance load	5.76 Ω (0.89 p.u.)

VI. EXPERIMENTAL RESULTS

To verify the effectiveness of the improved-SHE-scheme-based active compensation method on the 5th line current harmonic attenuation as shown in Fig. 9, plenty of experiments have been carried out on a 10 kVA/208 V/60 Hz PWM CSR prototype with the parameters listed in Table II.

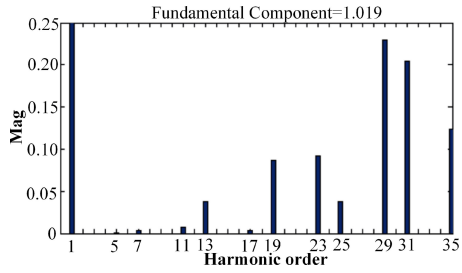

Fig. 14. Harmonic content of a 11-pulse SHE PWM pattern.

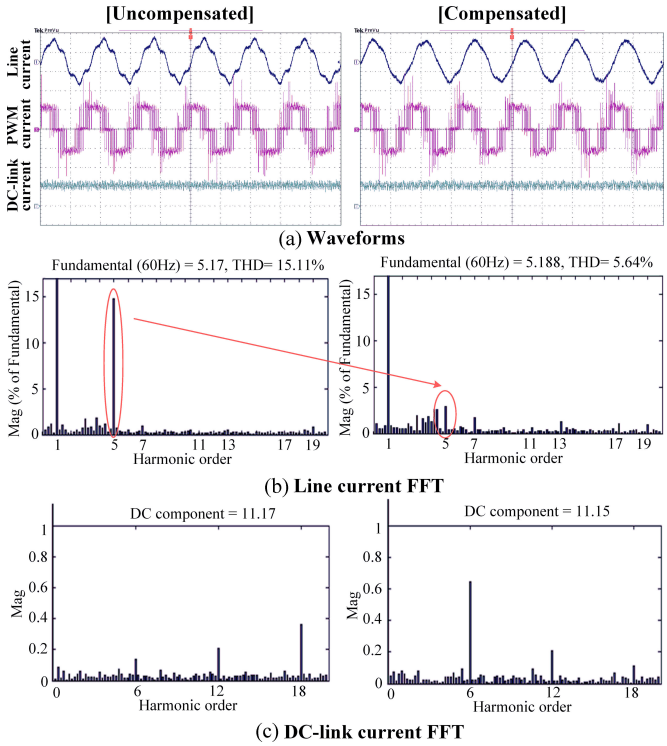

Fig. 15. Steady-state compensation performance under 1% 5th grid voltage harmonic (11-pulse SHE-based compensation). (i_s: 5 A/div, i_w: 10 A/div, i_{dc}: 10 A/div, time: 10 ms/div).

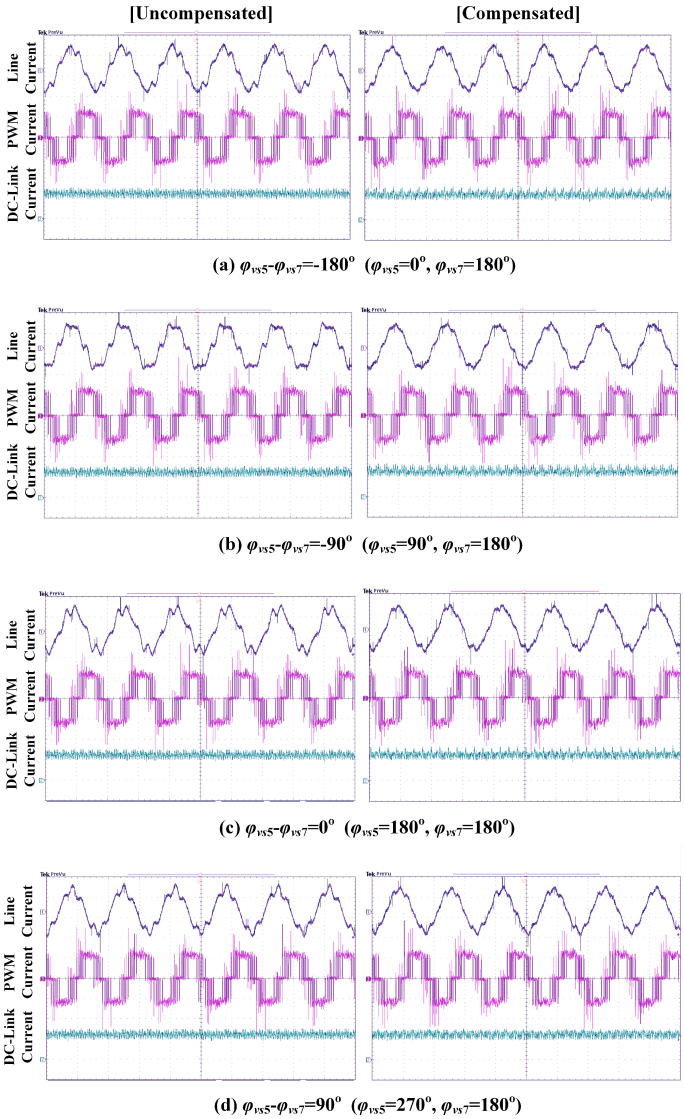

Fig. 16. Current waveforms before and after using the proposed method under different 5th (1%) and 7th (1%) grid voltage harmonics' initial phases (11-pulse SHE-based compensation).

A. Eleven-Pulse SHE-Based Compensation

Following the design criteria discussed in Section V, an 11-pulse SHE pattern is designed by using optimization method [16], [21] (weighing coefficient on each order harmonic is selected according to the design criteria in Section V). The harmonic content of the 11-pulse SHE pattern is shown in Fig. 14. The steady-state and dynamic compensation performance of the proposed method based on the 11-pulse SHE pattern are tested as follows.

To test the steady-state compensation performance, the grid voltage is programmed to contain 1% 5th harmonic at first. Fig. 15 shows the experimental results before and after using the proposed method. It can be observed that the 5th line current is greatly reduced and there is no significant increase on the other order line current harmonics. To further verify its effectiveness, the grid voltage is programmed to contain 1% 5th and 1% 7th harmonics. Fig. 16 shows the current waveforms under four different sets of the 5th grid voltage harmonic's initial phase (φ_{vs5}) and the 7th grid voltage harmonic's initial phase (φ_{vs7}). It can be observed that, after using the proposed compensation method, the distortion of line current are highly reduced. Fig. 17 shows the FFT analysis of line current in Fig. 16. We can observe that the 5th line current harmonic can be well attenuated under all conditions and no significant increase is introduced on the other line current harmonics.

To test the dynamic performance, two experiments are carried out. Fig. 18 shows the transient of applying the proposed method. Fig. 19 shows the transient of 1% step change of the 5th grid voltage harmonic under the adoption of the proposed method. It can be observed from the three figures that the dynamics of the proposed method is fast and the dc-link current control is not affected.

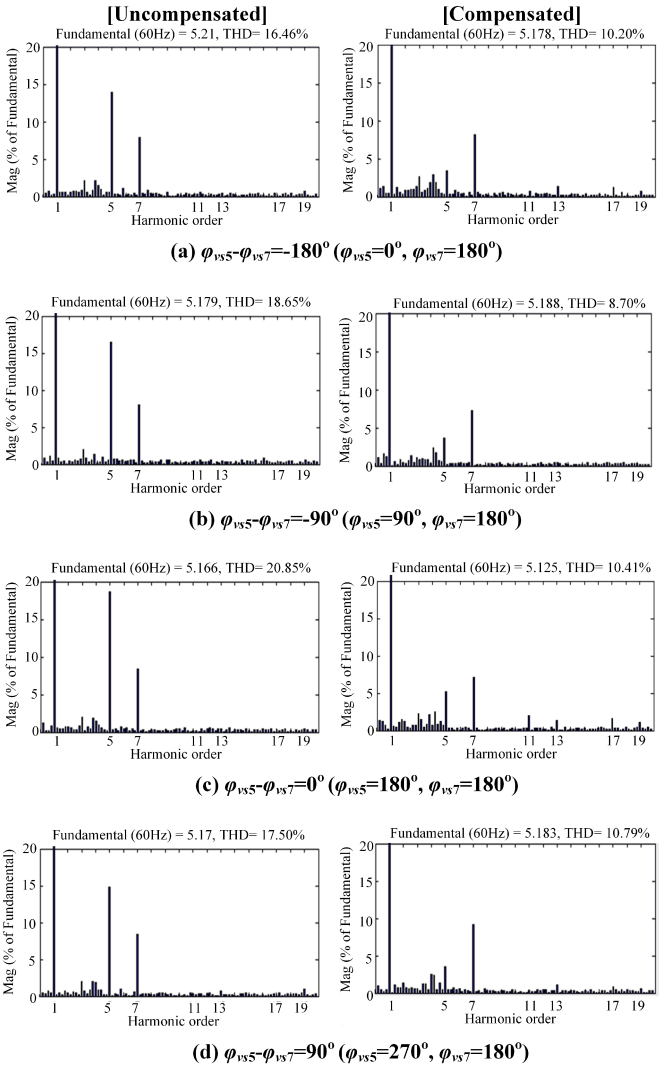

Fig. 17. FFT analysis of line current in Fig. 16.

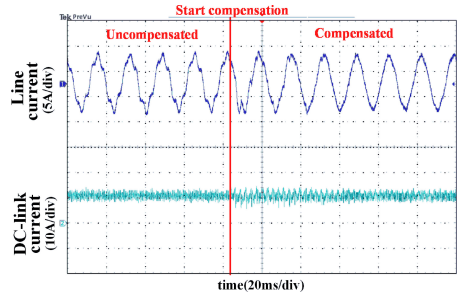

Fig. 18. Transient of starting compensation (11-pulse SHE-based compensation).

B. Nine-Pulse SHE-Based Compensation

In the previously mentioned tests, the proposed compensation method is based on a 11-pulse SHE pattern. The pulse numbers of SHE PWM pattern can be further reduced from 11 pulses to 9 pulses with harmonic content shown in Fig. 20. The 9-pulse SHE pattern is designed by the traditional SHE design scheme, fully elimination of certain low-order harmonics

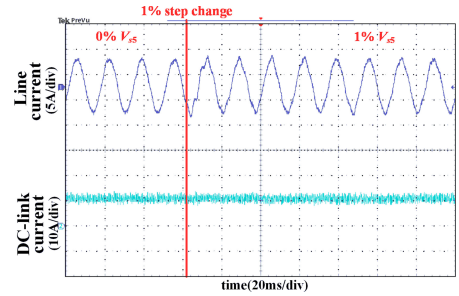

Fig. 19. Transient of 1% change of 5th grid voltage harmonic (11-pulse SHE-based compensation).

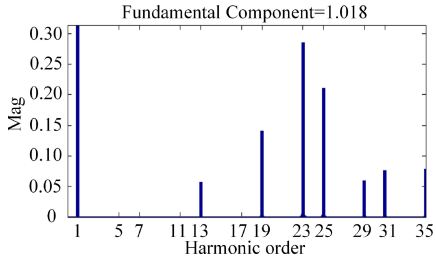

Fig. 20. Harmonic content of 9-pulse SHE PWM pattern.

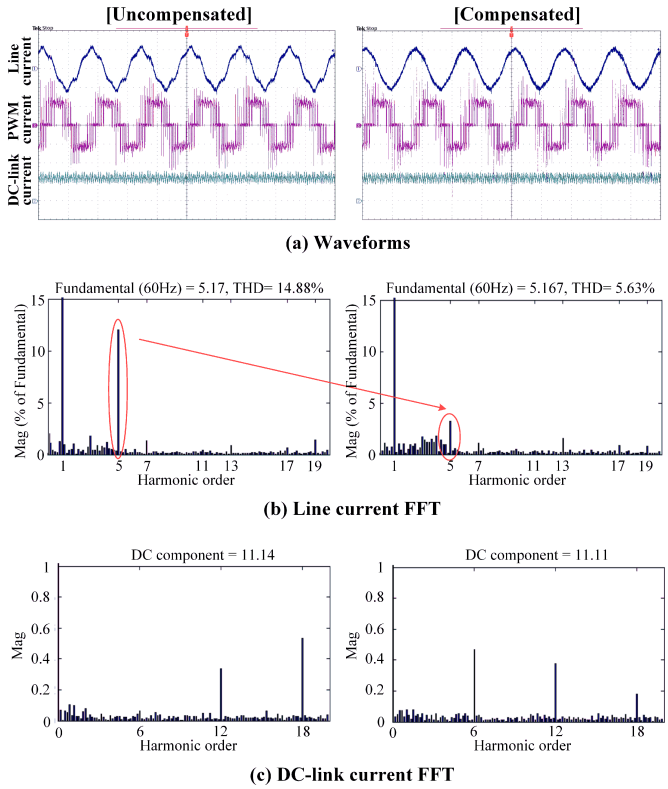

Fig. 21. Steady-state compensation performance under 1% 5th grid voltage harmonic (9-pulse SHE-based compensation). (i_s: 5 A/div, i_w: 10 A/div, i_{dc}: 10 A/div, time: 10 ms/div).

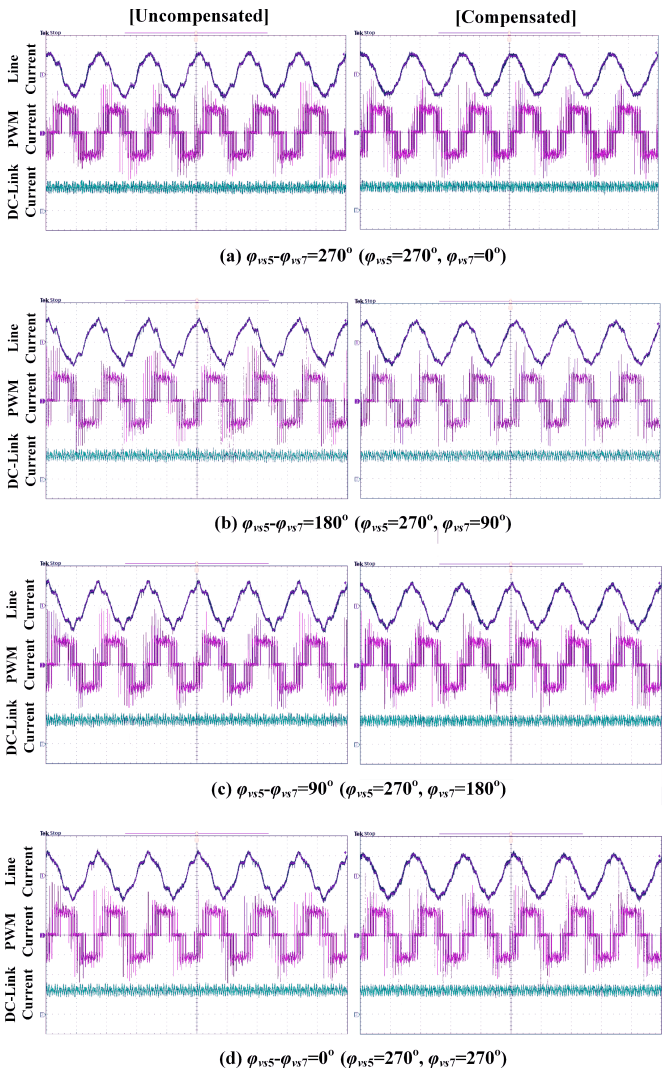

Fig. 22. Current waveforms before and after using the proposed compensation method under different 5th (1%) and 7th (1%) grid voltage harmonics' initial phases (9-pulse SHE-based compensation).

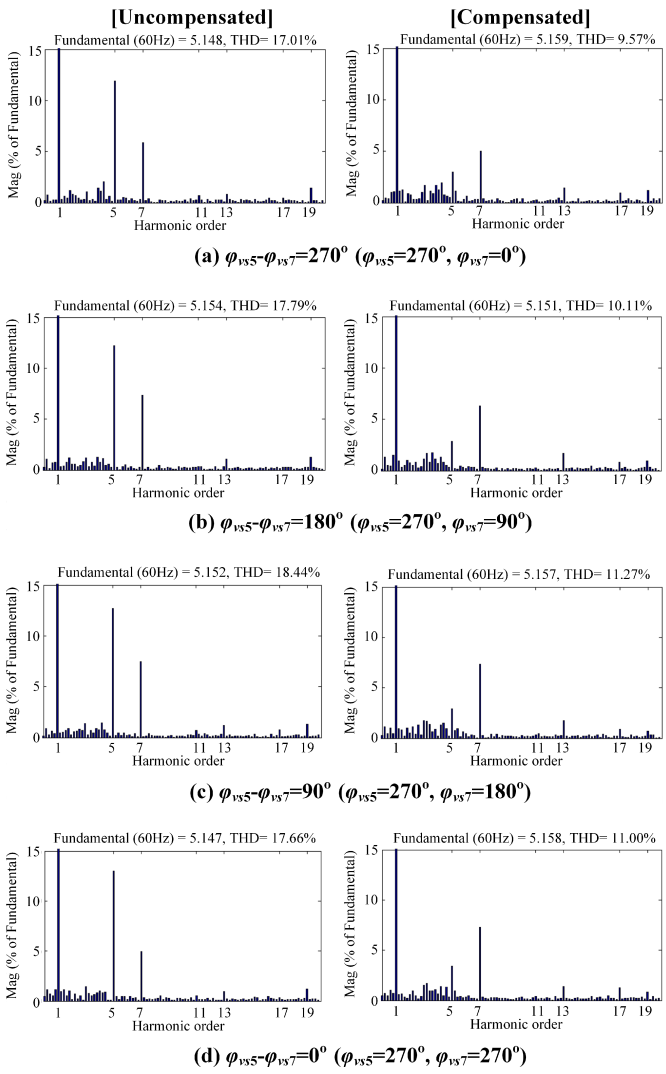

Fig. 23. FFT analysis of line current in Fig. 22.

as mentioned in Section V. In this situation, the 5th, 7th, 11th, and 17th harmonics are fully eliminated (note that the four lowest order harmonics, 5th, 7th, 11th, and 13th, cannot be fully eliminated simultaneously in theory). Comparing Fig. 20 with Fig. 14, we can observe that the 13th, 19th, 23rd, and 25th harmonics of the 9-pulse SHE pattern are higher than the previous 11-pulse SHE pattern. However, the following experimental results show that their influence on compensation performance is ignorable.

The same tests of steady-state compensation performance are conducted with the proposed compensation method based on the 9-pulse SHE pattern. Fig. 21 is obtained under 1% 5th grid voltage harmonic. Figs. 22 and 23 are obtained under 1% 5th and 1% 7th grid voltage harmonics, and four different sets of their initial phase. Compared with the experimental results of compensation based on 11-pulse SHE pattern, the proposed compensation method based on 9-pulse SHE pattern shows a good performance as well. It proves that the proposed method can be well combined with the traditional SHE scheme.

VII. Conclusion

An improved SHE scheme with online harmonic compensation is presented in this paper to enable the active compensation capability of the high-power PWM converters. The proposed method actively produces the expected harmonics in PWM pattern through introducing an alternating signal in the SHE phase angle. Such alternating signal can be obtained by a simple algebraic calculation according to the expected PWM harmonics, and it alters the predefined SHE pattern in real time to produce the corresponding harmonics through the converter. Compared to the SHC scheme based active compensation, the proposed improved SHE scheme not only saves the effort on the creation of lookup table, but also realizes the real-time compensation without any delay introduced. In this paper, an implementation example of the improved-SHE-scheme-based active

compensation to actively attenuate the 5th line current harmonic in high-power PWM CSR system is provided, and the experimental results have verified the effectiveness of the proposed method. Although the PWM CSR system is used as an example, according to the earlier analysis, the proposed method that improves the traditional SHE PWM scheme through jittering its phase angle has a great potential to be used in both the high-power current-source converters and voltage-source converters for more flexible control of the converter's output harmonic pattern. It is also important to note that this real-time online harmonic compensation can realize the grid harmonic control using the grid interfacing high-power converters with a very low switching frequency. This can be a very important ancillary functions in future grid interfacing high-power converter systems, such as PV plant, wind farm, STATCOM, HVDC, etc.

REFERENCES

[1] B. Wu, *High-Power Converters and AC Drives*. New York, NY, USA: Wiley, 2006, pp. 219–283.

[2] J. C. Wiseman and B. Wu, "Active damping control of a high-power PWM current-source rectifier for line-current THD reduction," *IEEE Trans. Ind. Electron.*, vol. 52, no. 3, pp. 758–764, Jun. 2005.

[3] Z. Wang, B. Wu, D. Xu, and N. R. Zargari, "A current-source-converter-based high-power high-speed PMSM drive with 420Hz switching frequency," *IEEE Trans. Ind. Electron.*, vol. 59, no. 7, pp. 2970–2981, Jul. 2012.

[4] Y. W. Li, M. Pande, N. R. Zargari, and B. Wu, "An input power factor control strategy for high-power current-source induction motor drive with active front-end," *IEEE Trans. Power Electron.*, vol. 25, no. 2, pp. 352–359, Feb. 2010.

[5] Y. W. Li, M. Pande, N. R. Zargari, and B. Wu, "Power-factor compensation for PWM CSR-CSI-fed high-power drive system using flux adjustment," *IEEE Trans. Power Electron.*, vol. 24, no.12, pp. 3014–3019, Dec. 2009.

[6] Y. W. Li, M. Pande, N. R. Zargari, and B. Wu, "DC-link current minimization for high-power current-source motor drives," *IEEE Trans. Power Electron.*, vol. 24, no. 1, pp. 232–240, Jan. 2009.

[7] F. Liu, B. Wu, N. R. Zargari, and M. Pande, "An active damping method using inductor-current feedback control for high-power PWM current-source rectifier," *IEEE Trans. Power Electron.*, vol. 26, no. 9, pp. 2580–2587, Sep. 2011.

[8] M. H. Bierhoff and F. W. Fuchs, "Active damping for three-phase PWM rectifiers with high-order line-side filters," *IEEE Trans. Ind. Electron.*, vol. 56, no. 2, pp. 371–379, Feb. 2009.

[9] J. D. Ma, B. Wu, N. R. Zargari, and S. C. Rizzo, "A space vector modulated CSI-based AC drive for multimotor applications," *IEEE Trans. Power Electron.*, vol. 16, no. 4, pp. 535–544, Jul. 2001.

[10] Y. Sato and T. Kataoka, "A current-type PWM rectifier with active damping function," *IEEE Trans. Ind. Appl.*, vol. 32, no. 3, pp. 533–541, May 1996.

[11] Z. Wang, B. Wu, D. Xu, and N. R. Zargari, " Dynamic capacitor voltage control of high power current-source converter fed PMSM drives for LC resonance suppression," in *Proc. IEEE ISIE*, 2010, pp. 792–797.

[12] S. A. S Grogan, D. G. Holms, and B. P. McGrath, "High performance voltage regulation of current-source inverters," *IEEE Trans. Power Electron.*, vol. 26, no. 9, pp. 2439–2448, Sep. 2011.

[13] J. Dannehl, F. W. Fuchs, S. Hansen, and P. Bach, "Investigation of active damping approaches for PI-based current control of grid-connected pulse width modulation converters with LCL filters," *IEEE Trans. Ind. Appl.*, vol. 46, no. 4, pp. 1509–1517, Jul. 2010.

[14] Y. W. Li, "Control and resonance damping of voltage-source and current-source converters with LC filters," *IEEE Trans. Ind. Electron.*, vol. 56, no. 5, pp. 1511–1521, May 2009.

[15] J. R. Wells, B. M. Nee, P. L. Chapman, and P.T. Krein, "Selective harmonic control: A general problem formulation and selected solutions," *IEEE Trans. Power Electron.*, vol. 20, no. 6, pp. 1337–1345, Nov. 2005.

[16] J. Napoles, J. I. Leon, R. Portillo, L. G. Franquelo, and M. A. Aguirre, "Selective harmonic mitigation technique for high-power converters," *IEEE Trans. Ind. Electron.*, vol. 57, no. 7, pp. 2315–2323, Jul. 2010.

[17] C. Namuduri and P. C. Sen, "Optimal pulsewidth modulation for current-source inverters," *IEEE Trans. Ind. Appl.*, vol. 22, no. 6, pp. 1052–1068, Nov. 1986.

[18] H. Zhou, Y. W. Li, N. R. Zargari, G. Cheng, R. Ni, and Y. Zhang, "Selective harmonic compensation (SHC) PWM for grid-interfacing high-power converters," *IEEE Trans. Power Electron.*, vol. 29, no. 3, pp. 1118–1127, Mar. 2014.

[19] R. Ni, Y. W. Li, Y. Zhang, N. R. Zargari, and G. Cheng, "Virtual impedance based selective harmonic compensation (VI-SHC) PWM for current-source rectifiers," *IEEE Trans. Power Electron.*, vol. 29, no. 7, pp. 3346–3356, Jul. 2014.

[20] D. G. Holmes and T. A. Lipo, *Pulse Width Modulation for Power Converters Principles and Practice*. New York, NY, USA: IEEE, 2003, pp. 409–411.

[21] V. G. Agelidis, A. Balouktsis, and I. Balouktsis, "On applying a minimization technique to the harmonic elimination PWM control: The bipolar waveform," *IEEE Power Electron. Lett.*, vol. 2, no. 2, pp. 41–44, Jun. 2004.

Ye Zhang (S'13) received the B.Eng. and M.Sc. degrees in electrical engineering from Beihang University, Beijing, China, in 2008 and 2011, respectively. He is currently working toward the Ph.D. degree in electrical power engineering in the Department of Electrical and Computer Engineering, University of Alberta, Edmonton, AB, Canada.

His current research interests include current-source converters, ac motor drives, and control system design.

Yun Wei Li (S'04–M'05–SM'11) received the B.S.E. degree in electrical engineering from Tianjin University, Tianjin, China, in 2002, and the Ph.D. degree from Nanyang Technological University, Singapore, in 2006.

In 2005, he was a Visiting Scholar with Aalborg University, Denmark. From 2006 to 2007, he was a Postdoctoral Research Fellow at Ryerson University, Canada. In 2007, he was at Rockwell Automation Canada, and later in the same year, he joined the Department of Electrical and Computer Engineering, University of Alberta, Canada, where he is currently an Associate Professor. His current research interests include distributed generation, microgrid, renewable energy, high-power converters, and electric motor drives.

Dr. Li is an Associate Editor for the IEEE TRANSACTIONS ON POWER ELECTRONICS and the IEEE TRANSACTIONS ON INDUSTRIAL ELECTRONICS. He was a Guest Editor for the IEEE TRANSACTIONS ON INDUSTRIAL ELECTRONICS SPECIAL SESSION ON DISTRIBUTED GENERATION AND MICROGRIDS. He received the 2013 Richard M. Bass Outstanding Young Power Electronics Engineer Award from IEEE Power Electronics Society.

Navid R. Zargari (S'91–M'95–SM'03) received the B.Eng. degree from Tehran University, Tehran, Iran, in 1987, and the M.A.Sc. and Ph.D. degrees from Concordia University, Montreal, QC, Canada, in 1991 and 1995, respectively.

He has been with Rockwell Automation Canada since November 1994, first as a Senior Designer and currently as the Manager of the Medium Voltage R&D Department. For the past 18 years, he has been involved with simulation, analysis, and design of power converters for medium-voltage AC drives. His current research interests include power converter topologies and their control aspects, power semiconductors and renewable energy sources. He has coauthored more than 50 research papers and holds 12 US patents. In 2011, he coauthored a book *Power Conversion and Control of Wind Energy Systems*.

Dr. Zargari is registered as a Professional Engineer in the Province of Ontario. He received the Premier's Innovation Award in 2009.

Zhongyuan Cheng (M'06) received the M.A.Sc. degree in electrical and computer engineering from Ryerson University, Toronto, ON, Canada, in 2005, and the Ph.D. degree in electrical engineering from Huazhong University of Science and Technology, Wuhan, China, in 1995.

In 2006, he joined Rockwell Automation Canada, Cambridge, ON, Canada. He is currently involved in medium-voltage drive topology, power electronics design and control. His current research interests include the integration and application aspects such as drive-utility interaction, MV drives in generator system and drive stability in various applications, and design aspects such as pulsewidth modulation, power converter topology, and component sizing.